



OPTICAL PARAMETER OF THE TIN SELENIDE NANOPARTICLES PREPARED BY AQUEOUS SOLUTION METHOD

Dr. R. J. Parmar*

Department of Physics, Sheth M. N. Science College, Patan, Gujarat, India.

*Corresponding Author

Dr. R. K. Parmar

Department of Physics, Govt. Science College, Vadnagar, Gujarat, India.

Dr. R. J. Pathak

R.R.Mehta science & C.L.Parikh commerce college, Palanpur, Gujarat, India.

ABSTRACT Tin selenide (SnSe) is a significant IV-VI semiconductor and one of the materials with the most potential uses. The chemical precipitation process in deionizer water has been used to create tin selenide (SnSe) powder. A spectrophotometer was used to examine the powder's optical characteristics. It was discovered that the indirect optical band gap was 1.5 eV.

KEYWORDS : SnSe nanoparticles, aqueous solution method, Optical parameter.

INTRODUCTION

A semiconductor in the IV-VI family is tin selenide (SnSe). It is receiving attention and growing interest because of its important and distinctive qualities. SnSe nanoparticles have been employed in memory switching devices, light-emitting or laser-emitting diodes, and infrared generation and detection. Several techniques were used to create SnSe nanoparticles, including brush plating, aqueous solution, self-propagating high temperature synthesis, Bridgman, solid-state reaction, and solid-state metathesis. In addition, I employ the chemical precipitation approach, which is a fairly simple procedure that doesn't require a computer or a high temperature. Depending on the deposition conditions, this time-consuming procedure allows for a better alignment of the crystallites with an enhanced grain structure. The morphological analysis and preparation of the tin selenide powder made using a straightforward chemical process are presented in this research.

EXPERIMENTAL DETAILS:

Every chemical used in this mixture was of AR grade. The purity of Alpha essar is 99.99%. The chemical system's precursors for the ions Sn^{2+} and Se^{2-} are tin chloride and selenium oxide. Using a magnetic stirrer, the SnCl_2 and SeO_2 solutions were combined drop by drop for 30 minutes, resulting in the precipitation of SnSe in the solution. To separate the SnSe nanoparticles from this precipitation, it was centrifuged for 15 minutes at 3000 rpm. After being separated, the SnSe nanoparticles were repeatedly cleaned with ethanol and then heated to 100°C for an hour to produce a dry powder. Measurements of the synthesized nanoparticles were conducted using optical absorption spectroscopy in the 200–2500 nm wave length region. (Perkin Elmer Lambda-19)



Figure. Photograph of synthesized SnSe nanoparticles

UV-VIS: Figure 1. Shows the variation of the prepared tin selenide nanoparticles. Optical absorption spectra of as synthesized nanoparticles were taken with the help of UVVIS-NIR spectrophotometer in the wavelength range of 200 nm – 2500 nm. It is good for absorbing the photons since the nanoparticles have a wide range of absorption from the NIR to the UV.

SnSe nanocrystalline powders formed by the chemical precipitation process have an absorption peak at the incident wavelength of 200 nm, according to a thorough analysis of these absorption spectra.

The absorption coefficient (α) can be computed from the absorption data by applying the formula

$$\alpha = 2.303 A/t.$$

The relationship between the incident photon energy ($h\nu$) and the absorption coefficient (α) can be expressed as [15],

$$(ah\nu)^{-1} = B(h\nu - E_g)$$

Exponent "n" is dependent on the type of transition, "B" is a constant, and "E_g" is the material's optical gap. 'n' may have values 1/2, 2, 3/2 and 3 corresponding to the allowed direct, allowed indirect, forbidden direct and forbidden indirect transitions respectively. The value of n determine by following method.

The value of n was calculated using the plot of Log ($ah\nu$) vs Log (E_g). Slope of this straight line gives the value of 'n' and we determine nature of transition take place in our nanocrystalline powders grown by chemical precipitation method. Whether it is direct or indirect transition. From the Fig.2 it is seen that slope of straight line ≈ 2.11 . From this value we can say that in our grown nanocrystalline powders Allowed Indirect transition takes place.

We plot graph of $(ah\nu)^{1/2} \rightarrow h\nu$ we determine exact optical band gap of our grown nanocrystalline powders as shown in Figure 3. The optical Bandgap of the SnSe nanoparticles E_g = 1.5591.

Furthermore, optical parameter like extinction coefficient (K) and refractive index (n) are important parameters for characterizing photonic materials. Values of 'n' and 'K' of grown nanocrystalline powders from transmission and reflection spectra using the relation,

$$K = \frac{\alpha\lambda}{4\pi}$$

$$n = 1 + \sqrt{R/1-R}$$

The percentage of light lost as a result of scattering and absorption by the penetrating medium per unit distance is known as the extinction coefficient. Fig.5 illustrates how the extinction coefficient falls as the visible wavelength range increases.

The decrease in extinction coefficient with increase in certain value of wavelength shows that the fraction of light lost due to scattering and absorbance decreases.

The variation of refractive index η with wavelength of nanocrystalline powders of SnSe is shown in Fig. 4 The greater the visible wavelength range, the lower the refractive index. The value of the refractive index η increases above the visual range. The normal dispersion law describes how the refractive index varies.

The general trend of variation in refractive index and extinction coefficient spectra with wavelength is found to remain fairly the same

but inversely.

On the other hand, the frequency dependence of the real part ϵ_r and imaginary part ϵ_i of the complex dielectric constants are related to K and n have been determined through the following equations,

$$\epsilon_r = n^2 - K^2$$

$$\epsilon_i = 2nK$$

Where ϵ_r (real part) is the dielectric constant and ϵ_i (imaginary part) is the dielectric loss factor.

Fig.5 & 6 shows that the variation of imaginary part and real part of dielectric constant for SnSe nanoparticles. At lower value of energy, value of imaginary part of dielectric constant (ϵ_i) first starts to decrease and after particular energy of radiation it reaches to maximum value.

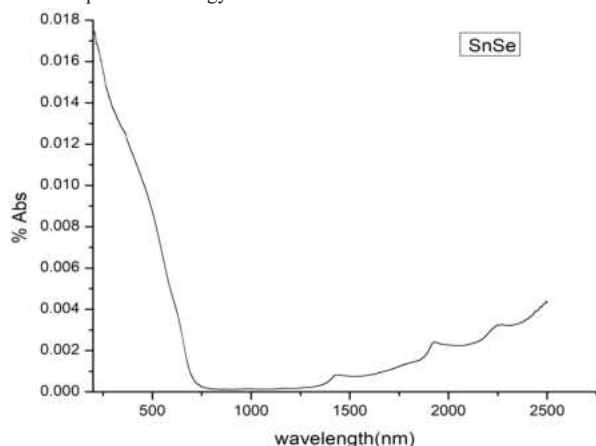


Figure.1 Optical absorbance spectra SnSe nanoparticles

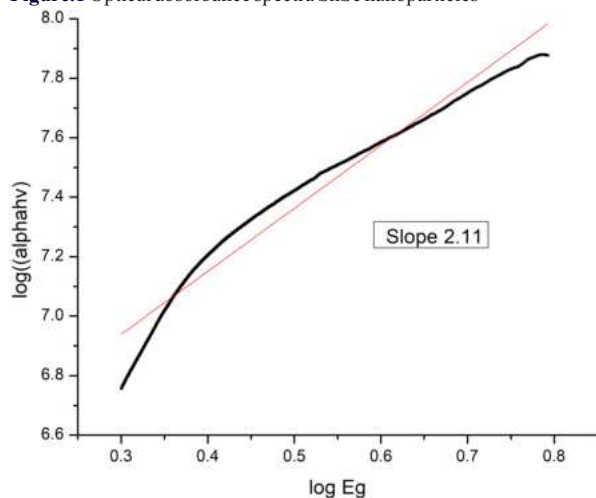


Figure.2 Plot of $\log(\alpha h\nu) \rightarrow \log(E_g)$

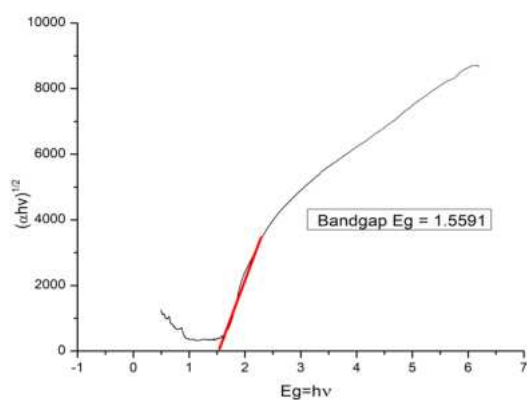


Figure.3 Plot of $(\alpha h\nu)^{1/2} \rightarrow h\nu$

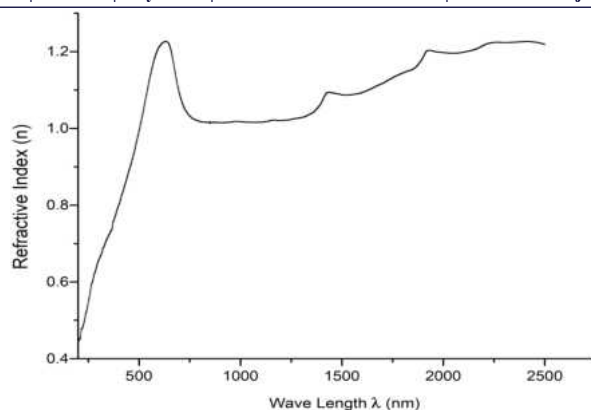


Figure.4 Refractive index as a function of wavelength

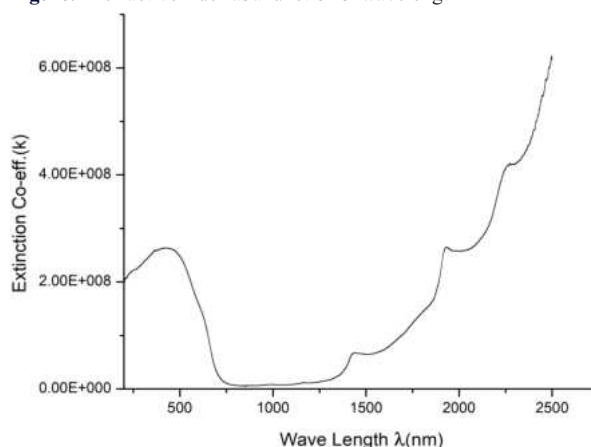


Figure.5 Extinction Co-efficient (K) as a function of wavelength

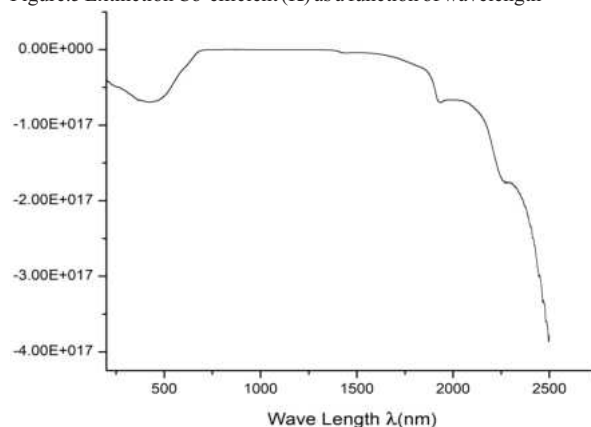


Figure.6 Dielectric Constant Real Part (ϵ_r) as a function of wavelength.

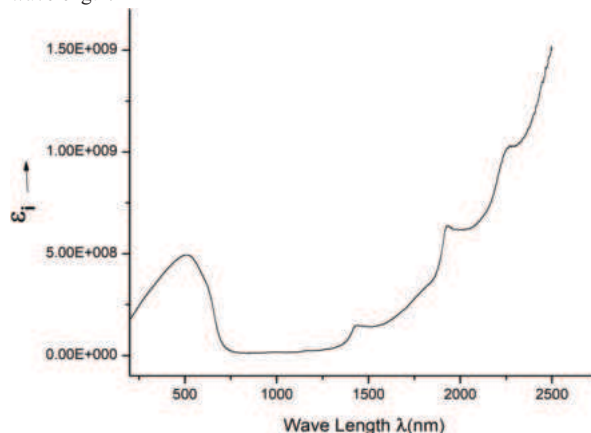


Figure.7 Dielectric Constant Imaginary Part (ϵ_i) as a function of wavelength.

CONCLUSIONS

In this study, a simple chemical route for Tin selenide nanoparticles has been described. The technique is simple, cost-effective and requires less monitoring. In the optical study, the band gap was found to be forbidden indirect and about 1.5591 eV. In Optical parameter, The Extinction coefficient decreases with the increase in the visible wavelength range. Refractive index decreases with increase in visible wavelength range. Above the visible range, the value of refractive index η is increased. Variation in refractive index follows the normal dispersion law.

REFERENCES:

- [1] Zulkarnain Zainal, Saravanan Nagalingam, Anuar Kassim, Mohd Zabir Hussein and Wan Mahmood Mat Yanus, *Solar Energy Materials and Solar Cells*, 81,261-268, 2004.
- [2] Zweibel K.,*Solar Energy Mater, Solar Cells*, 63, 375-386 2000.
- [3] L. Seligson and J.Arnold, *J.Amer. Chem. Soc.*, 115, 8214-8220 1993.
- [4] Batt v.p., Giresam K. and Pandya G.R., *J. Crystal Growth*, 96, 649-651 1989.
- [5] Yi H. and Moore J.J., *J. Mater. Sci.*, 25, 1159-1168 1990.
- [6] Parkin I.P., *Chem. Soc. Rev.*, 25, 199-207 1996.
- [7] Subramaniam B., Sanjeeviraja C. and Jayachandran M., *J. Crystal Growth*, 234, 421-426 2002.
- [8] Dong-Hau Kuo, Wei-Di Huang, Ying-Sheng Huang, Jiun-De Wu, Yan-Jih Lin, *Thin Solid Films*, 518(24), 7218 2010.
- [9] N. Kumar, V. Sharma, U. Parihar, R. Sachdeva, N. Padha, C.J. Panchal, *J. Nano-Electron. Phys.* 3 No.1, 117 2011.
- [10] Ziaul Raza Khan, M. Zulfequar, Mohd. Shahid Khan, *Chalcogenide Letters*, 7, 431-438 2010.
- [11] N.A. Okereke, A. J. Ekpunobi, *Journal Of Optoelectronics and Biomedical Materials*, 3(3), 69 2011.
- [12] Hoffmon, M., Martin, S., Choi, W., & Bahnemann, D. 1995. "Environmental applications of semiconductor photo catalysis," *Chemical Review*, Vol. 95, PP. 69-96.
- [13] Wikipedia: Bandgap definition and diagram, <http://en.wikipedia.org/wiki/Bandgap>
- [14] *Fundamentals of Molecular Spectroscopy*; C. N. Banwell University of Sussex, 3rd edition, May 1983.
- [15] N. Kumar, V. Sharma, N. Padha, N. M. Shah, M. S. Desai, C. J. Panchal, I. Yu. Protsenko, *Cryst. Res. Technol.*, 45 (1), (2010), 53.